PHYSICAL REVIEW D **87,** 055005 (2013)

Yukawa unification predictions for the LHC

Archana Anandakrishnan,[1] Stuart Raby,[1] and Akın Wingerter[2]

[1]*Department of Physics, The Ohio State University, 191 West Woodruff Avenue, Columbus, Ohio 43210, USA*

[2]*Laboratoire de Physique Subatomique et de Cosmologie, UJF Grenoble 1, CNRS/IN2P3, INPG, 53 Avenue des Martyrs, F-38026 Grenoble, France*

(Received 6 December 2012; published 6 March 2013)

This paper is divided into two parts. In the first part we analyze the consequences, for the LHC, of gauge and third-family Yukawa coupling unification with a particular set of boundary conditions defined at the grand unification scale. We perform a global χ^2 analysis including the observables M_W, M_Z, G_F, $\alpha_{\rm em}^{-1}$, $\alpha_s(M_Z)$, M_t, $m_b(m_b)$, M_τ, BR$(B \to X_s\gamma)$, BR$(B_s \to \mu^+\mu^-)$, and M_h. The fit is performed in the minimal supersymmetric Standard Model in terms of nine grand unification-scale parameters, while $\tan\beta$ and μ are fixed at the weak scale. Good fits suggest an upper bound on the gluino mass, $M_{\tilde{g}} \lesssim 2$ TeV. This constraint comes predominantly from fitting the bottom-quark and Higgs masses (assuming a 125 GeV Higgs). Gluinos should be visible at the LHC in the 14 TeV run but they cannot be described by the typical simplified models. This is because the branching ratios for $\tilde{g} \to t\bar{t}\tilde{\chi}^0_{1,2}$, $b\bar{b}\tilde{\chi}^0_{1,2}$, $t\bar{b}\tilde{\chi}^-_{1,2}$, $b\bar{t}\tilde{\chi}^+_{1,2}$, $g\tilde{\chi}^0_{1,2,3,4}$ are comparable. Top squarks and sbottoms may also be visible. Charginos and neutralinos can be light, with the lightest supersymmetric particle predominantly bino-like. In the second part of the paper we analyze a complete three-family model and discuss the quality of the global χ^2 fits and the differences between the third-family analysis and the full three-family analysis for overlapping observables. We note that the light Higgs in our model couples to matter like the Standard Model Higgs. Any deviation from this would rule out this model.

DOI: 10.1103/PhysRevD.87.055005 PACS numbers: 12.60.Jv, 12.10.Dm, 12.15.Ff

I. INTRODUCTION

Gauge coupling unification in supersymmetric grand unified theories (SUSY GUTs) [1–6] provides an experimental hint for low energy SUSY. However, it does not significantly constrain the spectrum of supersymmetric particles. On the other hand, it has been observed that Yukawa coupling unification for the third generation of quarks and leptons in models, such as SO(10) or $SU(4)_c \times SU(2)_L \times SU(2)_R$, can place significant constraints on the SUSY spectrum in order to fit the top, bottom, and tau masses [7–11]. These constraints depend on the particular boundary conditions for sparticle masses chosen at the GUT scale (see, for example, Refs. [9,12,13], which consider different GUT-scale boundary conditions). In light of the present success of the LHC with the possible observation of the Higgs boson with mass of order 125 GeV and significant lower bounds on gluino and squark masses, it is a perfect time to review the viability of the constraints on the sparticle spectrum resulting from gauge and third-generation Yukawa coupling unification.[1] This is what we do in this paper. In part one of the paper, we perform a global χ^2 analysis assuming SO(10) boundary conditions for sparticle masses and nonuniversal Higgs masses, which we have called "just-so Higgs splitting." We fit the observables M_W, M_Z, G_F, $\alpha_{\rm em}^{-1}$, $\alpha_s(M_Z)$, M_t, $m_b(m_b)$, M_τ, BR$(B \to X_s\gamma)$, BR$(B_s \to \mu^+\mu^-)$, and M_h in terms of 11 arbitrary parameters. These fits then place significant constraints on the gluino mass.

In the second part of the paper we study a complete three-family model of quark and lepton Yukawa couplings at the GUT scale [16,17] which is based on an SO(10) GUT with a $D_3 \times [U(1) \times \mathbb{Z}_2 \times \mathbb{Z}_3]$ family symmetry. This model was shown to give good fits to precision electroweak data, including quark, charged lepton, and neutrino masses and mixing angles (see most recently the global χ^2 analysis in Ref. [18]). In light of the observation of $\sin^2\theta_{13}$ it is again a perfect time to reanalyze this model. We are also able to compare the third-family Yukawa unification analysis with the three-family analysis which now includes hierarchical Yukawa matrices with unification of the (3, 3) element of the Yukawa matrices. Hence, off-diagonal elements in the Yukawa matrices give small corrections to exact Yukawa unification.

The paper is organized as follows. In Sec. II, we present the SO(10) model. In Sec. III, we present the procedure used in the paper for analyzing the model. In Sec. IV, we consider a model with gauge coupling unification and only the Yukawa couplings for the third family, which are assumed to unify at the GUT scale. We perform a global χ^2 analysis fitting the relevant low-energy observables. In Sec. V, we extend the analysis to all three families of quarks and leptons using a particular SO(10) GUT model. In this case, we look for the minimum values of χ^2 for five different choices of the universal squark and slepton mass, m_{16}, defined at the GUT scale, M_G. Finally, the summary and conclusions are given in Sec. VI.

[1]For other analyses in this direction, see Refs. [14,15].

 © 2013 American Physical Society

II. THE MODEL

A. Third-family model

Fermion masses and quark mixing angles are manifestly hierarchical. The simplest way to describe this hierarchy is with Yukawa matrices, which are also hierarchical. Moreover, the most natural way to obtain the hierarchy is in terms of effective higher-dimension operators of the form

$$W \supset \lambda 16_3 10 16_3 + 16_3 10 \frac{45}{M} 16_2 + \cdots \tag{1}$$

This version of SO(10) models has the nice features that it only requires small representations of SO(10), has many predictions and can, in principle, find a UV completion in string theory. The only renormalizable term in W is $\lambda 16_3 10 16_3$, which gives Yukawa coupling unification

$$\lambda = \lambda_t = \lambda_b = \lambda_\tau = \lambda_{\nu_\tau} \tag{2}$$

at $M_{\rm GUT}$. Note, one *cannot* predict the top mass due to large SUSY threshold corrections to the bottom and tau masses, as shown in Refs. [19–21]. These corrections are of the form

$$\delta m_b/m_b \propto \frac{\alpha_3 \mu M_{\tilde g} \tan\beta}{m_{\tilde b}^2} + \frac{\lambda_t^2 \mu A_t \tan\beta}{m_{\tilde t}^2} + \text{log corrections}. \tag{3}$$

So instead we use Yukawa unification to predict the soft SUSY-breaking masses. In order to fit the data, we need

$$\delta m_b/m_b \sim -2\%. \tag{4}$$

We take $\mu\ M_{\tilde g} > 0$, and thus we need $\mu\ A_t < 0$. For a short list of references on this subject, see Refs. [7–11,14,22–24].

Given the following GUT-scale boundary conditions—namely, universal squark and slepton masses, m_{16}, the universal cubic scalar parameter, A_0, universal gaugino masses, $M_{1/2}$, and nonuniversal Higgs masses or "just-so" Higgs splitting, m_{H_u}, m_{H_d} or $m^2_{H_{u(d)}} = m^2_{10}[1 - (+)\Delta^2_{m_H}]$—we find that fitting the top, bottom, and tau mass forces us into the region of SUSY-breaking parameter space with

$$\begin{aligned} A_0 &\approx -2m_{16}, \qquad m_{10} \approx \sqrt{2} m_{16}, \\ m_{16} &> \text{few TeV}, \qquad \mu, M_{1/2} \ll m_{16}, \end{aligned} \tag{5}$$

and, finally,

$$\tan\beta \approx 50. \tag{6}$$

In addition, radiative electroweak symmetry breaking requires $\Delta^2_{m_H} \approx 13\%$, with roughly half of this coming naturally from the renormalization-group running of neutrino Yukawa couplings from M_G to $M_{N_\tau} \sim 10^{13}$ GeV [9].

It is very interesting that the above region in SUSY parameter space results in an inverted scalar mass hierarchy at the weak scale with the third-family scalars significantly lighter than the first two families [25]. This has the nice property of suppressing flavor-changing neutral current and CP-violating processes. These results depend solely on SO(10) Yukawa unification for the third family. In order to demonstrate this, we perform a separate analysis with only third-family observables (Sec. IV) and then a complete three-family analysis (Sec. V).[2]

B. Full three-family model

We now consider a complete three-family SO(10) model for fermion masses and mixing, including neutrinos [16–18]. The model also includes a $D_3 \times [\mathrm{U}(1) \times \mathbb{Z}_2 \times \mathbb{Z}_3]$ family symmetry which is necessary to obtain a predictive theory of fermion masses by reducing the number of arbitrary parameters in the Yukawa matrices. Consider the superpotential generating the effective fermion Yukawa couplings:

$$W_{\rm ch fermions} = \lambda 16_3 10 16_3 + 16_a 10 \chi_a + \bar\chi_a \left(M_\chi \chi_a + 45 \frac{\phi_a}{\hat M} 16_3 + 45 \frac{\tilde\phi_a}{\hat M} 16_a + \boldsymbol{A} 16_a \right), \tag{7}$$

where **45** is an SO(10) adjoint field which is assumed to obtain a vacuum expectation value (VEV) in the $B - L$ direction, M_χ is a linear combination of an SO(10) singlet and adjoint, and the index $a = 1, 2$. Its VEV $M_\chi = M_0(1 + \alpha X + \beta Y)$ gives mass to Froggatt-Nielsen states [26]. Here, X and Y are elements of the Lie algebra of SO(10) with X in the direction of the U(1) which commutes with SU(5) and Y the standard weak hypercharge, and α, β are arbitrary constants which are fit to the data. $\hat M$ is an SO(10) invariant mass scale which in principle could be obtained by integrating out additional Froggatt-Nielsen states. Note that both M_0 and $\hat M$ are assumed to be above the GUT scale. ϕ_a, $\tilde\phi_a$, $\boldsymbol{A}$ are SO(10) singlet "flavon" fields, $\boldsymbol{A}$ is a nontrivial one-dimensional representation under D_3, and $\bar\chi_a$, χ_a are a pair of Froggatt-Nielsen states transforming as a $\overline{\mathbf{16}}$ and **16** under SO(10). The so-called flavon fields are *assumed* to obtain VEVs of the form

$$\langle \phi_a \rangle = \begin{pmatrix} \phi_1 \\ \phi_2 \end{pmatrix}, \qquad \langle \tilde\phi_a \rangle = \begin{pmatrix} 0 \\ \tilde\phi_2 \end{pmatrix}. \tag{8}$$

[2]The large Yukawa coupling for the third family is the driving force for the inverted scalar mass hierarchy. However, the particular boundary conditions of Eq. (5) were shown to maximize the effect.

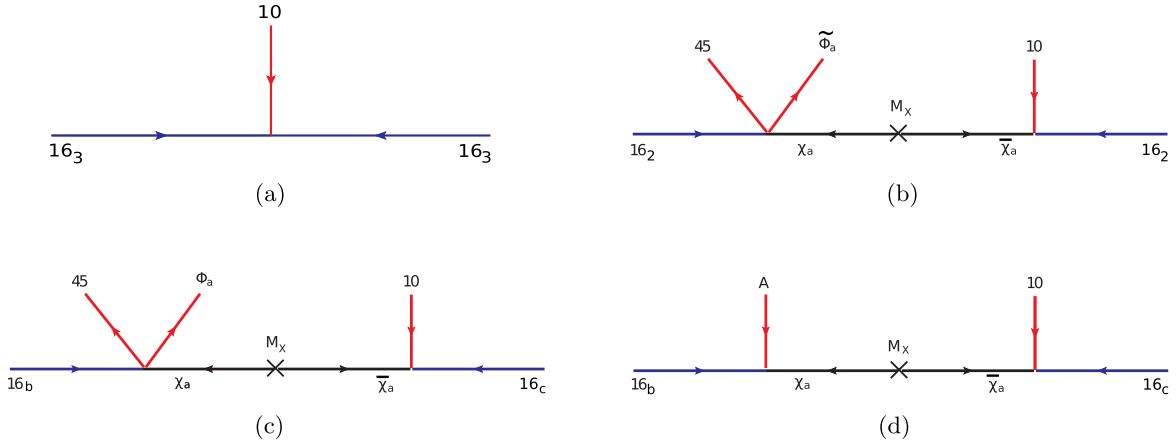

FIG. 1 (color online). (a) Renormalizable mass term for the third family that gives rise to the (3, 3) element of the Yukawa matrix. (b) Effective operator that generates the (2, 2) element of the Yukawa matrix. (c) Effective operators that generate the off-diagonal Yukawa couplings: $(b, c) = (3, 2), (2, 3), (3, 1)$, or $(1, 3)$. (d) Effective operators that generate the off-diagonal Yukawa couplings: $(b, c) = (2, 1)$ or $(1, 2)$. The effective fermion mass operators were obtained after integrating out the Froggatt-Nielsen massive states. Here, a runs from 1 to 2.

After integrating out the Froggatt-Nielsen states one obtains the effective fermion mass operators in Fig. 1.

Inserting the flavon VEVs, one then obtains Yukawa matrices for up-quarks, down-quarks, charged leptons, and neutrinos given by

$$Y_u = \begin{pmatrix} 0 & \epsilon'\rho & -\epsilon\xi \\ -\epsilon'\rho & \tilde{\epsilon}\rho & -\epsilon \\ \epsilon\xi & \epsilon & 1 \end{pmatrix}\lambda,$$
$$Y_d = \begin{pmatrix} 0 & \epsilon' & -\epsilon\xi\sigma \\ -\epsilon' & \tilde{\epsilon} & -\epsilon\sigma \\ \epsilon\xi & \epsilon & 1 \end{pmatrix}\lambda, \qquad (9)$$
$$Y_e = \begin{pmatrix} 0 & -\epsilon' & 3\epsilon\xi \\ \epsilon' & 3\tilde{\epsilon} & 3\epsilon \\ -3\epsilon\xi\sigma & -3\epsilon\sigma & 1 \end{pmatrix}\lambda,$$

with

$$\xi = \phi_2/\phi_1, \qquad \tilde{\epsilon} \propto \tilde{\phi}_2/\hat{M}, \qquad \epsilon \propto \phi_1/\hat{M},$$
$$\epsilon' \sim (\mathbf{A}/M_0), \qquad \sigma = \frac{1+\alpha}{1-3\alpha}, \qquad \rho \sim \beta \ll \alpha, \qquad (10)$$

and

$$Y_\nu = \begin{pmatrix} 0 & -\epsilon'\omega & \frac{3}{2}\epsilon\xi\omega \\ \epsilon'\omega & 3\tilde{\epsilon}\omega & \frac{3}{2}\epsilon\omega \\ -3\epsilon\xi\sigma & -3\epsilon\sigma & 1 \end{pmatrix}\lambda, \qquad (11)$$

with $\omega = 2\sigma/(2\sigma - 1)$ and a Dirac neutrino mass matrix given by

$$m_\nu \equiv Y_\nu \frac{v}{\sqrt{2}} \sin\beta. \qquad (12)$$

From Eqs. (9) and (11) one can see that the flavor hierarchies in the Yukawa couplings are encoded in terms of the four complex parameters ρ, σ, $\tilde{\varepsilon}$, ξ and the additional real ones ε, ε', λ. These matrices contain seven real parameters and four arbitrary phases. Note, the superpotential [Eq. (7)] has many arbitrary parameters. However, at the end of the day the effective Yukawa matrices have much fewer parameters. This is good, because we then obtain a very predictive theory. Also, the quark mass matrices accommodate the Georgi-Jarlskog mechanism, such that $m_\mu/m_e \approx 9m_s/m_d$. This is a result of the **45** VEV in the $B - L$ direction.

We then add three real Majorana mass parameters for the neutrino see-saw mechanism. The antineutrinos obtain GUT-scale masses by mixing with three SO(10) singlets (N_a for $a = 1, 2$ and N_3), transforming as a D_3 doublet and singlet, respectively. The full superpotential is given by $W = W_{\text{ch fermions}} + W_{\text{neutrino}}$, with

$$W_{\text{neutrino}} = \overline{16}(\lambda_2 N_a 16_a + \lambda_3 N_3 16_3) + \frac{1}{2}(S_a N_a N_a + S_3 N_3 N_3), \qquad (13)$$

where the fields S_a, S_3 are additional flavon fields whose VEVs provide Majorana masses for the states N_a, N_3. We assume $\overline{16}$ obtains a VEV, v_{16}, in the right-handed neutrino direction, and $\langle S_a \rangle = M_a$ for $a = 1, 2$ and $\langle S_3 \rangle = M_3$. The effective neutrino mass terms are given by

$$W = \nu m_\nu \bar{\nu} + \bar{\nu} V N + \frac{1}{2} N M_N N, \qquad (14)$$

with

TABLE I. The model is defined by three gauge parameters, α_G, M_G, ϵ_3; one large Yukawa coupling, λ; five SUSY parameters defined at the GUT scale, m_{16} (universal scalar mass for squarks and sleptons), $M_{1/2}$ (universal gaugino mass), m_{H_u}, m_{H_d} (up and down Higgs masses), and A_0 (universal trilinear scalar coupling); μ, $\tan\beta$ are obtained at the weak scale by consistent electroweak symmetry breaking. The full three-family model has additional off-diagonal Yukawa couplings, and includes three right-handed neutrino masses.

Sector	Third-family analysis	No.	Full three-family analysis	No.
Gauge	α_G, M_G, ϵ_3	3	α_G, M_G, ϵ_3	3
SUSY (GUT scale)	m_{16}, $M_{1/2}$, A_0, m_{H_u}, m_{H_d}	5	m_{16}, $M_{1/2}$, A_0, m_{H_u}, m_{H_d}	5
Textures	λ	1	ϵ, ϵ', λ, ρ, σ, $\tilde{\epsilon}$, ξ	11
Neutrino		0	M_{R_1}, M_{R_2}, M_{R_3}	3
SUSY (EW scale)	$\tan\beta$, μ	2	$\tan\beta$, μ	2
Total number		11		24

$$V = v_{16}\begin{pmatrix} 0 & \lambda_2 & 0 \\ \lambda_2 & 0 & 0 \\ 0 & 0 & \lambda_3 \end{pmatrix}, \quad M_N = \mathrm{diag}(M_1, M_2, M_3) \tag{15}$$

all assumed to be real. Finally, upon integrating out the heavy Majorana neutrinos we obtain the 3×3 Majorana mass matrix for the light neutrinos in the lepton flavor basis given by

$$\mathcal{M} = U_e^T m_\nu M_R^{-1} m_\nu^T U_e, \tag{16}$$

where the effective right-handed neutrino Majorana mass matrix is given by

$$M_R = V M_N^{-1} V^T \equiv \mathrm{diag}(M_{R_1}, M_{R_2}, M_{R_3}), \tag{17}$$

with

$$M_{R_1} = (\lambda_2 v_{16})^2/M_2, \qquad M_{R_2} = (\lambda_2 v_{16})^2/M_1, \qquad M_{R_3} = (\lambda_3 v_{16})^2/M_3. \tag{18}$$

III. PROCEDURE

A. Renormalization-group equations

The model parameters, summarized in Table I, are defined at the grand unification scale M_G with the exception of $\tan\beta$ and μ, which are defined at the electroweak scale. At the GUT scale, $\alpha_G \equiv \alpha_1(M_G) = \alpha_2(M_G)$ and $\alpha_3(M_G) = \alpha_G(1 + \epsilon_3)$, where ϵ_3 is the GUT-scale threshold correction[3] necessary to fit the strong coupling to experimental data at the electroweak scale, M_Z. These three gauge parameters, the 11 Yukawa textures (described in Sec. II B), five SUSY boundary conditions, and three real neutrino mass parameters allow us to completely define the model at the GUT scale and derive all the parameters of the minimal supersymmetric standard model (MSSM).

[3]Without presenting a complete GUT we leave ϵ_3 as a free parameter. In this way, our analysis will also apply to orbifold GUTs or string compactifications with a scale of order M_G.

First, the GUT-scale parameters are renormalization group equation (RGE)-evolved to the right-handed neutrino (RHN) scale where the RHNs are integrated out (see Fig. 2). The right-handed neutrinos have three different scales associated with them, and the most relevant one is the third-family RHN that is mostly responsible for splitting the up- and down-type Higgs masses. We therefore choose to integrate out all the right-handed neutrinos at one single scale, $M_{N_\tau} = M_{R_3}$.

Below the scale of the RHNs, we use the two-loop MSSM RGEs for both dimensionful and dimensionless parameters. Ideally, one should evolve all parameters to the scale of the heavy scalars (m_{16} in this case, as shown in Fig. 2) and integrate them out and proceed to evolve to the weak scale using an effective theory without the first two generations of scalars. We choose an alternative approach and use the two-loop MSSM RGE[4] evolution down to the weak scale and correct for the additional running by including one-loop threshold corrections to the relevant observables.[5] This approximation eliminates the need to define multiple effective theories. In our analysis, we have been careful to take into account the corresponding threshold corrections for all observables.

B. Electroweak observables

At the weak scale, we calculate the SUSY spectrum and the SUSY threshold corrections to the fermion masses and Cabibbo-Kobayashi-Maskawa (CKM) matrix elements. Especially in the large-$\tan\beta$ regime, these SUSY threshold corrections are very important for the down-type quarks and charged leptons and can be at the percent level in Yukawa-unified SUSY models [21].

[4]In scenarios with heavy scalars, it has been shown that the two-loop contributions to the third-generation scalars can lead to dramatic consequences, like driving the stop mass-squared negative [27], and thus it is important to include the two-loop RGEs in scenarios such as that discussed here.

[5]For the calculation of the Higgs mass, we define an effective theory at the scale M_{SUSY} and interface our calculation with the code used by the authors of Ref. [28].

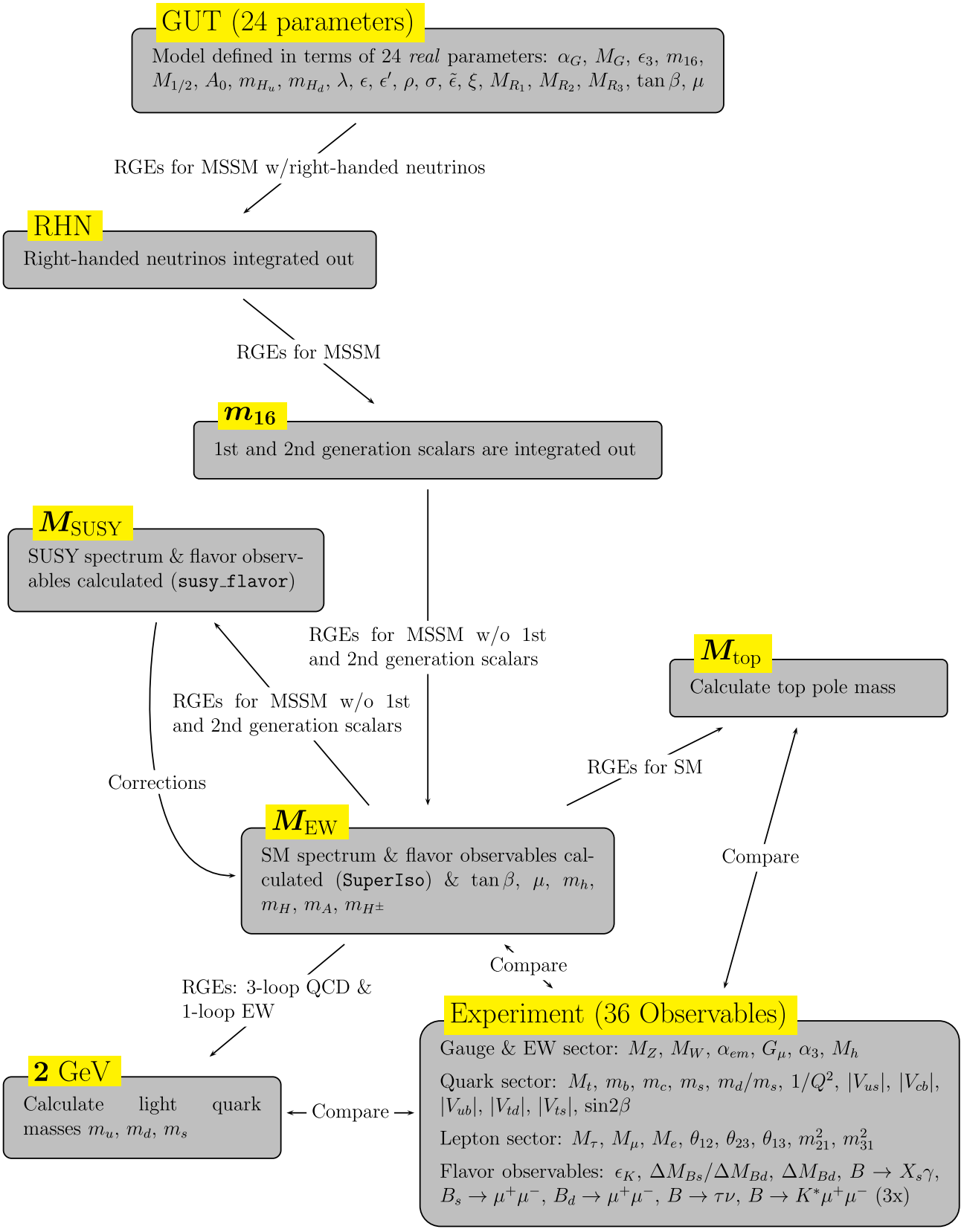

FIG. 2 (color online). This schematic shows the steps that must be employed to evolve a GUT model to the low energies and to calculate observables at the relevant scales to compare with experimental data. Note that we use threshold corrections instead of integrating out the two families of scalars from the particle spectrum.

We then use the threshold-corrected fermion masses to determine the tree-level masses for the squarks and sleptons. In addition, we also determine the one-loop pole mass for the gluino and the CP-odd Higgs mass. The precision electroweak observables M_Z, M_W, G_μ, $\alpha_{\rm em}^{-1}(M_Z)$, and $\alpha_s(M_Z)$ are calculated including one-loop threshold corrections, using the procedure described in Refs. [29,30]. Following the prescription in Ref. [29], the condition for consistent radiative electroweak symmetry breaking is also imposed at the weak scale, and for this, we use the physical Z pole mass. The parameter μ is fixed by this procedure via a separate χ^2 minimization, and in the process, we fit the Z mass precisely to the physical Z pole mass. In the calculation of M_Z and M_W, we only include the one-loop corrections from the third-family scalars, since the first two generations of scalars are integrated out at m_{16}. We assign a theoretical uncertainty of 0.5% to our calculation of the electroweak observables (except for M_Z) due to the approximate treatment of thresholds described above. We also assign a 1% theoretical uncertainty to our calculation of G_μ, since we neglect the SUSY vertex and box diagrams. Finally, to compare to experiment, $\alpha_{\rm em}$ is evolved to zero momentum transfer.

C. Charged fermion masses and mixing angles

Below M_Z, we integrate out all SUSY partners and electroweak gauge bosons to obtain an effective $\mathrm{SU}(3)\times\mathrm{U}(1)_{\rm em}$ low-energy theory. We use one-loop QED and three-loop QCD RGEs to renormalize to the appropriate scales and calculate the low-energy observables. We fit the top-quark pole mass, and the bottom- and charm-quark $\overline{\rm MS}$ masses are calculated at their respective masses. All the other light quark masses are calculated at the scale of 2 GeV. We fit seven observables relevant to quark masses, three charged lepton masses, and six CKM observables. The theoretical uncertainty in their calculation is again estimated to be 0.5%. Since the light quark masses are not measured to very high precision, we choose to fit multiple correlated observables. These include the $\overline{\rm MS}$ strange-quark mass, the mass ratio m_d/m_s, and the mass ratio Q defined in the Particle Data Group [31] as

$$Q^2=\frac{m_s^2-1/4(m_u+m_d)^2}{m_d^2-m_u^2},\quad \text{or equivalently,}\quad \left(\frac{m_u}{m_d}\right)^2+\frac{1}{Q^2}\left(\frac{m_s}{m_d}\right)^2=1. \tag{19}$$

The CKM matrix is calculated from the left and right mixing matrices by diagonalizing the Yukawa matrices and including the SUSY threshold corrections. Six CKM observables ($|V_{us}|$, $|V_{ub}|$, $|V_{cb}|$, $|V_{td}|$, $|V_{ts}|$, and $\sin2\beta$) are included in our global-fit analysis. To account for the inconsistencies in the inclusive and exclusive measurements of $|V_{ub}|$ and $|V_{cb}|$, we allow our result to be within the experimental error from both the inclusive and the exclusive measurement. The pole masses in the lepton sector are calculated with one-loop electromagnetic threshold corrections.

To execute the steps elaborated so far, we use the code MATON, originally developed by Radovan Dermíšek to study Yukawa unification in the SO(10) model with $D_3\times[\mathrm{U}(1)\times\mathbb{Z}_2\times\mathbb{Z}_3]$ family symmetry [17]. MATON has been restructured and extended appropriately to adapt to the current analysis.

D. Higgs mass

The recent observation of the Higgs boson at the LHC [32,33] will allow us to highly constrain the parameter space of the model. Flavor constraints have already pushed the first two generations of scalars of Yukawa-unified SUSY models $\gtrsim 10$ TeV [34]. In contrast, the third-family scalars have masses of about a few TeV, purely by the effects of RGE running. The hierarchy between the first two and the third generations alleviates the constraints from flavor physics and CP-violating observables, and at the same time eases the large fine-tuning in models with heavy scalars. In addition to the TeV-range scalars, the large A-terms make it easy to obtain a Higgs mass of about 125 GeV. We integrate out all the scalars (including the third-generation squarks and sleptons) below the scale $M_{\rm SUSY}$, and calculate the Higgs boson mass using the dedicated code by the authors of Ref. [28], which is best suited to our case where the sfermions are very heavy. Given the boundary conditions

$$\mu(M_Z),\quad M_1(M_{\rm SUSY}),\quad M_2(M_{\rm SUSY}),\quad M_3(M_{\rm SUSY}),\quad M_{\rm SUSY},\quad \tan\beta,\quad A_t(M_{\rm SUSY})$$

at the scale $M_{\rm SUSY}=\sqrt{M_{\tilde t_1}\times M_{\tilde t_2}}$, (where M_1, M_2, M_3 are the gaugino masses at the scale $M_{\rm SUSY}$), the routine [28] determines the Higgs mass by calculating the corrections to the Higgs quartic coupling:

$$M_h=\sqrt{\frac{\lambda(M_{\rm SUSY})}{\sqrt{2}G_\mu}}(1+\delta^{\rm SM}(M_{\rm SUSY})+\delta^{\chi}(M_{\rm SUSY})). \tag{20}$$

δ^χ are the contributions from chargino and neutralino diagrams. The quartic coupling $\lambda(M_{\rm SUSY})$ is given by

$$\lambda(M_{\rm SUSY})=\frac{1}{4}(g^2+g'^2)+\frac{3h_t^4}{8\pi^2}\left[\left(1-\frac{g^2+g'^2}{8h_t^2}\right)\frac{X_t^2}{M_{\rm SUSY}^2}-\frac{X_t^4}{12M_{\rm SUSY}^4}\right]. \tag{21}$$

We have to point out an important difference in our approach. The conventional method is to use the SM

inputs of M_Z, G_μ, $\alpha_{\rm em}^{-1}(M_Z)$, $\alpha_s(M_Z)$, M_t, $m_b(m_b)$, and M_τ to determine the gauge and the Yukawa couplings at the scales $M_{\rm SUSY}$ and further constrain the GUT-scale parameters. We instead like to predict these low-energy observables and constrain the GUT-scale parameter space based on a global χ^2 fit to the data. In our calculation of the Higgs mass, we take the gauge and Yukawa couplings as input at the scale $M_{\rm SUSY}$, obtained from RGE evolution using MATON, and calculate the Higgs mass using these inputs. The approach we adopt here is purely top-down. We have adapted the routine [28] to suit this line of analysis. Nevertheless, we have compared the spectrum we obtain from MATON with that from SOFTSUSY[6] [35] and find good agreement.

E. Neutrino sector

We are fitting five observables in the neutrino sector: the mixing angles θ_{12}, θ_{23}, θ_{13}, and the mass-squared differences $\Delta m_{31} \equiv m_3^2 - m_1^2$ and $\Delta m_{21} \equiv m_2^2 - m_1^2$ (cf. Table II). The most dramatic change in the experimental determination of the neutrino parameters in recent years comes from the Daya Bay and Reno collaborations [40,41], which have confirmed that $\theta_{13} \sim 9^\circ$ is indeed large. Moreover, there are tentative hints that θ_{23} is not maximal [42,43]. Whereas Ref. [42] sees a preference at $\sim 2\sigma$–3σ for the first octant, i.e., $\theta_{23} < 45^\circ$, Ref. [43] finds an equal probability for θ_{23} being larger or smaller than 45°. In the following, we will be using the best-fit values and the 3σ uncertainties quoted by the NUFIT collaboration [43], which are in agreement with Ref. [42] at 3σ.

F. Flavor physics

The strongest constraints on the model come from B-physics. For calculating the flavor observables, we use two publicly available codes, namely SUSY_FLAVOR [44] and SUPERISO [45,46]. Since the boundary conditions that we impose at the GUT scale may generate large off-diagonal and in general complex entries at the low scale, SUSY_FLAVOR is better adapted to our needs. Note that SUSY_FLAVOR, in contrast to comparable programs that calculate similar processes, does not assume minimal flavor violation, and allows for general, full three-family, complex soft parameters. This is particularly important in our case, since we are calculating several CP-violating observables and need to take into account[7] the complex phases in the soft parameters. Hence, SUSY_FLAVOR is our default choice for all flavor observables with the following exceptions. For $B \to X_s\gamma$, we use SUPERISO, since SUSY_FLAVOR does not include the next-to-next-to-leading-order SM corrections. We have verified that the discrepancy between SUSY_FLAVOR and SUPERISO in the parameter space that is of interest to us is at most 10% and typically less than 7%. Also, we use SUPERISO for the observables connected to the decay process $B \to K^* \mu^+ \mu^-$, since SUSY_FLAVOR does not provide them. It is important to note that SUPERISO has some built-in assumptions that prove to be too restrictive in our case, e.g., SUPERISO assumes all soft parameters to be real, and only takes the diagonal entries of the third-family trilinear couplings into account. As a consequence, we have assigned larger theoretical uncertainties to the values calculated by SUPERISO (see Table II). Additional sources of uncertainties in the flavor observables derive from the theoretical determination of the B-meson decay constant and from the experimental measurements of the CKM matrix elements.

LHCb has recently measured [39] the Br$(B_s \to \mu^+ \mu^-)$, which is in good agreement with the SM prediction. This pushes the CP-odd Higgs mass to a few TeV and hence leads to the Higgs decoupling limit. "Thus the light Higgs is predicted to be SM-like." The recent observation of zero-crossing in the forward-backward asymmetry of $B \to K^* \mu^+ \mu^-$ constrains the Wilson coefficient C_7 to be of the same sign as that in the SM. This imposes the additional constraint for the model that if $\mu > 0$, in order to satisfy the branching fraction observed in the process $B \to X_s\gamma$ the first two generations of scalars have to be heavier than at least 10 TeV.

G. Global fit

In the last step of our calculation, we construct a χ^2 function in terms of the 36 calculated observables (see Table II):

$$\chi^2 = \sum_i \frac{|y_i - y_i^{\rm data}|^2}{\sigma_i^2}. \tag{22}$$

y_i and $y_i^{\rm data}$ are the theoretical prediction and experimental measurement, respectively, for each observable. σ_i is the error on each observable, the theoretical and experimental errors added in quadrature. In the general case, we vary 23 parameters (see Table I and note that m_{16} is fixed in all the analyses) in order to fit 36 observables, which amounts to 12 (or 13 counting the separate fit to the Z pole mass) degrees of freedom (d.o.f.). We will consider the χ^2 per d.o.f. for the model as a qualitative measure of the goodness of fit. We will look at the pulls from the individual observables to assess the goodness of fit of the model.

Finding the global minimum for a model with 23 parameters is a formidable task. In the present analysis,

[6]Without making significant changes to SOFTSUSY or other publicly available codes, we find that we can only make rough comparisons of the spectra. This is because, to the best of our knowledge, most of the currently available codes do not handle complex parameters. In addition, many do not include right-handed neutrinos, and do not offer an easy way to implement the particular GUT-scale Yukawa texture of the model.

[7]We calculate the particle spectrum using MATON. To the best of our knowledge, there is currently no publicly available spectrum generator that fully takes into account all the complex phases of the MSSM.

TABLE II. The 36 observables that we fit and their experimental values. In the fourth column, we indicate the software package that gives us the theoretical prediction. In the last column, we show what we have assumed for the theoretical errors. Here, $Q^2 = (m_s^2 - 1/4(m_u + m_d)^2)/(m_d^2 - m_u^2)$ is defined on p. 657 of Ref. [31]. The number(s) in brackets after some of the values indicate the 1σ uncertainty in the last digit(s). Capital letters denote pole masses. We take LHCb results into account, but use the average given by Ref. [36]. All experimental errors are 1σ unless otherwise indicated. To account for the inconsistencies in the inclusive and exclusive measurements of $|V_{ub}|$ and $|V_{cb}|$, we allow our result to be within the experimental error from both the inclusive and the exclusive measurement. To minimize theoretical uncertainties, we fit the ratio $\Delta m_{B_s}/\Delta m_{B_d}$ and derive its error by the usual formula for error propagation using the value $\Delta m_{B_s} = (117.0 \pm 0.8) \times 10^{-10}$ MeV [31] and assuming no correlations between the errors. Finally, the Z mass is fit precisely via a separate χ^2 function solely imposing electroweak symmetry breaking.

Observable	Exp. value	Ref.	Program	Th. error
$\alpha_3(M_Z)$	0.1184 ± 0.0007	[31]	MATON	0.5%
$\alpha_{\rm em}$	1/137.035999074(44)	[31]	MATON	0.5%
G_μ	$1.16637876(7) \times 10^{-5}$ GeV^{-2}	[31]	MATON	1%
M_W	80.385 ± 0.015 GeV	[31]	MATON	0.5%
M_Z	91.1876 ± 0.0021	[31]	Input	0.0%
M_t	173.5 ± 1.0 GeV	[31]	MATON	0.5%
$m_b(m_b)$	4.18 ± 0.03 GeV	[31]	MATON	0.5%
$m_c(m_c)$	1.275 ± 0.025 GeV	[31]	MATON	0.5%
$m_s(2\ \text{GeV})$	95 ± 5 MeV	[31]	MATON	0.5%
$m_s/m_d(2\ \text{GeV})$	17–22	[31]	MATON	0.5%
Q	21–25	[31]	MATON	5%
$\lvert V_{us}\rvert$	0.2252 ± 0.0009	[31]	MATON	0.5%
$\lvert V_{ub}\rvert$	0.00377 ± 0.00085	[31]	MATON	0.5%
$\lvert V_{cb}\rvert$	0.04065 ± 0.00195	[31]	MATON	0.5%
$\lvert V_{td}\rvert$	0.00840 ± 0.0006	[31]	MATON	0.5%
$\lvert V_{ts}\rvert$	0.0429 ± 0.0026	[31]	MATON	0.5%
$\sin 2\beta$	0.679 ± 0.020	[31]	MATON	0.5%
M_τ	1776.82 ± 0.16 MeV	[31]	MATON	0.5%
M_μ	105.6583715(35) MeV	[31]	MATON	0.5%
M_e	0.510998928(11) MeV	[31]	MATON	0.5%
M_h	$125.3 \pm 0.4 \pm 0.5$ GeV	[32]	Ref. [28]	3 GeV
$\sin^2\theta_{12}$	0.27–0.34 (3σ range)	[37]	MATON	0.5%
$\sin^2\theta_{23}$	0.34–0.67 (3σ range)	[37]	MATON	0.5%
$\sin^2\theta_{13}$	0.016–0.030 (3σ range)	[37]	MATON	0.5%
Δm^2_{21}	$(7.00\text{–}8.09) \times 10^{-5}$ eV^2 (3σ range)	[37]	MATON	0.5%
Δm^2_{31}	$(2.27\text{–}2.69) \times 10^{-3}$ eV^2 (3σ range)	[37]	MATON	0.5%
BR$(b \to s\gamma)$	$(343 \pm 21 \pm 7) \times 10^{-6}$	[36]	SUPERISO	$(181\text{–}505) \times 10^{-6}$
BR$(B \to K^* \mu\mu)_{1 \le q^2 \le 6\text{GeV}^2}$	$(1.97 \pm 0.21) \times 10^{-7}$	[36]	SUPERISO	$(0.79\text{–}3.15) \times 10^{-7}$
BR$(B \to K^* \mu\mu)_{14.18 \le q^2 \le 16\text{GeV}^2}$	$1.20^{+0.11}_{-0.10} \times 10^{-7}$	[36]	SUPERISO	$(0.48\text{–}1.92) \times 10^{-7}$
$q_0^2(\text{A}_{\text{FB}}(B \to K^* \mu\mu))$	$4.9^{+1.1}_{-1.3}$ GeV^2	[38]	SUPERISO	4.86–4.94
BR$(B_s \to \mu^+\mu^-)$	3.2×10^{-9}	[39]	SUSY_FLAVOR	1.5×10^{-9}
BR$(B_u \to \tau\nu)$	$(166 \pm 33) \times 10^{-6}$	[36]	SUSY_FLAVOR	$(83\text{–}249) \times 10^{-6}$
BR$(B_d \to \mu^+\mu^-)$	$<8.1 \times 10^{-10}$	[36]	SUSY_FLAVOR	$<9.72 \times 10^{-10}$
Δm_{B_d}	$(3.337 \pm 0.033) \times 10^{-10}$MeV	[31]	SUSY_FLAVOR	$(2.67\text{–}4.00) \times 10^{-10}$
$\Delta m_{B_s}/\Delta m_{B_d}$	35.06 ± 0.42	[31]	SUSY_FLAVOR	28.05–42.07
ϵ_K	$(2.228 \pm 0.11) \times 10^{-3}$	[31]	SUSY_FLAVOR	$(2.00\text{–}2.45) \times 10^{-3}$

we minimize the χ^2 function using the Minuit package maintained by CERN [47]. Note that Minuit is not guaranteed to find the *global* minimum, but will in most cases converge on a local one. For that reason, we iterate $\mathcal{O}(100)$ times the minimization procedure for each set of input parameters, and in each step we take a different initial guess for the minimum (required by Minuit) so that we have a fair chance of finding the true minimum. This, of course, requires large computing resources, and to that end we have used the Ohio Supercomputer Center in Columbus and the "Centre de Calcul de l'Institut National de Physique Nucléaire et Physique des Particules" in Lyon.

TABLE III. SUSY spectrum corresponding to the benchmark points presented in the Appendix. The first two generations of scalars have mass of the order of m_{16}.

m_{16}	10 TeV	15 TeV	20 TeV	25 TeV	30 TeV
χ^2	49.65	31.02	26.58	27.93	29.48
M_A	2333	3662	1651	2029	2036
$m_{\tilde{t}_1}$	1681	2529	3975	4892	5914
$m_{\tilde{b}_1}$	2046	2972	5194	6353	7660
$m_{\tilde{\tau}_1}$	3851	5576	7994	9769	11620
$m_{\tilde{\chi}_1^0}$	133	134	137	149	167
$m_{\tilde{\chi}_1^+}$	260	263	279	309	351
$M_{\tilde{g}}$	853	850	851	910	1004

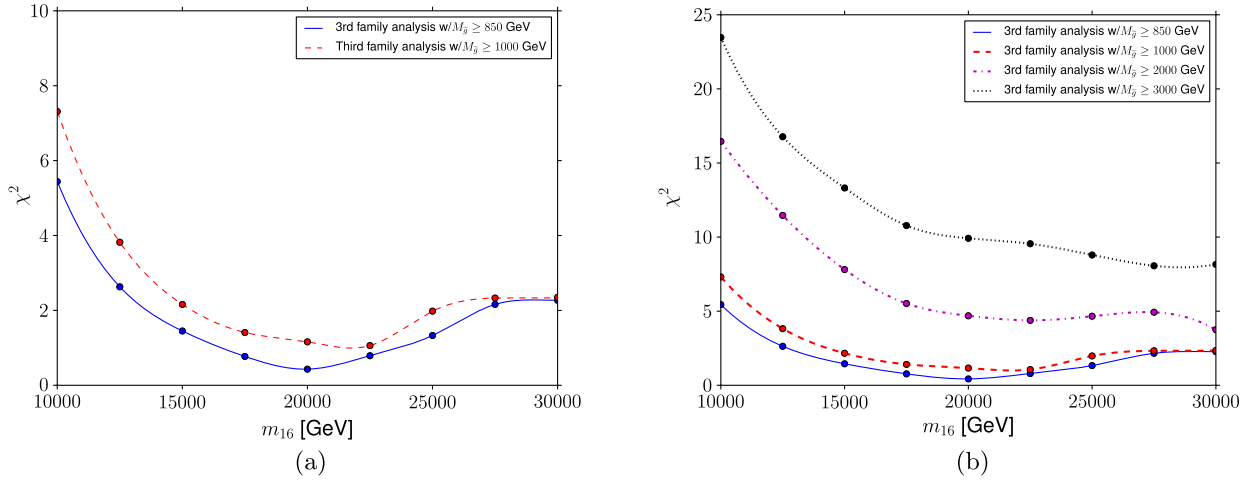

FIG. 3 (color online). (a) With increasing m_{16}, χ^2 first dramatically decreases, and after reaching a minimum around $m_{16} \simeq 20$ TeV, starts increasing again. (b) As we increase the lower bound on the gluino mass, we find that χ^2 dramatically increases for a constant m_{16}. χ^2 vs m_{16} for the third-family analysis. The filled circles correspond to minima of χ^2 for the values of m_{16} indicated on the x axis, where we have interpolated between them using cubic splines for ease of inspection. The curves correspond to different lower bounds on the gluino mass.

IV. THIRD-FAMILY ANALYSIS

In this section we analyze the consequences of Yukawa unification for the third family in the context of minimal SO(10) supersymmetric grand unification, defined by the superpotential term $W \supset \lambda 16_3 10 16_3$. The aim of this analysis is to study the SUSY spectrum, and we argue that the constraints on the SUSY spectrum come predominantly from the third family, the lightest Higgs mass, and the branching ratio $\mathrm{BR}(B_s \to \mu^+\mu^-)$. There are 24 parameters in total in the Dermisek-Raby model [16,17], and in this section we focus on 11 parameters (summarized in Table I) that are used to evaluate 11 low-energy observables: M_W, M_Z, G_F, $\alpha_{\mathrm{em}}^{-1}$, $\alpha_s(M_Z)$, M_t, $m_b(m_b)$, M_τ, $\mathrm{Br}(B \to X_s\gamma)$, $\mathrm{Br}(B_s \to \mu^+\mu^-)$, and the lightest Higgs mass, M_h. We specify the model with the full 24 parameters, but we only vary 11 in the minimization procedure to fit the 11 observables listed above. The irrelevant parameters for this analysis, namely, the neutrino parameters and the off-diagonal Yukawa textures, are set to constant values and do not enter into the minimization procedure.[8] Similarly, the low-energy observables connected to the first two families do not enter the χ^2 function. The effects of the off-diagonal Yukawa textures will be discussed in Sec. V.

Consider first the SUSY spectrum in our analysis. The first- and second-family squarks and sleptons have mass of order m_{16}, while top squarks, sbottoms, and staus are all significantly lighter. This is the inverted scalar mass hierarchy, which is a direct result of RG running. Nevertheless, gluinos are always lighter than the third-family squarks and sleptons, and the lightest charginos and neutralinos are even lighter. Note that the states $\tilde{\chi}^{\pm}$ and χ_2^0 are approximately degenerate. A detailed spectrum is given in Table III. Recent results from CMS and ATLAS give lower bounds on the gluino mass. These bounds are given in terms of the constrained MSSM or simplified models. The simplified models which are most relevant for our analysis are those in which (a) the third family of squarks and

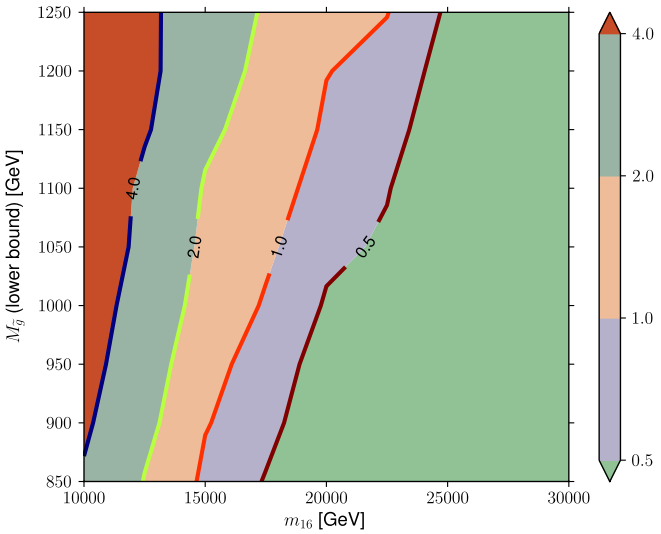

FIG. 4 (color online). The contribution of M_h to the global χ^2 as a function of the lower bound on the gluino mass (vertical axis) and the value of m_{16} (horizontal axis). The Higgs mass is mainly responsible for the steep increase of χ^2 observed in Fig. 3(a).

[8] In this section, when calculating flavor-violating observables, we use SUSY_FLAVOR with the experimental input values for the light fermion masses and mixing angles.

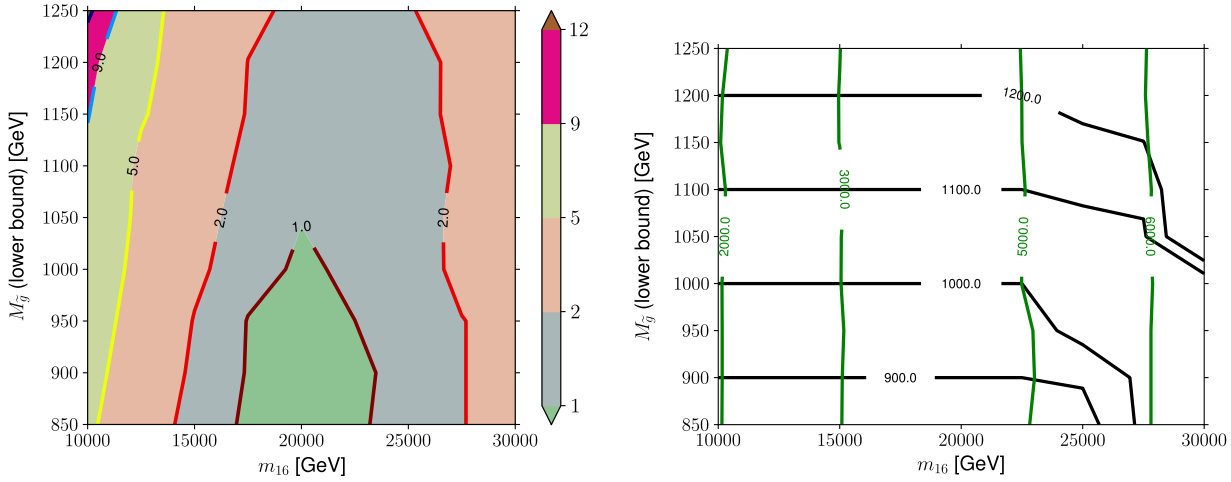

FIG. 5 (color online). The best χ^2 fits for the third-family analysis (left) and contours of constant gluino mass (roughly horizontal lines) and top squark masses (vertical lines) (right). Note, for larger values of $m_{16} \geq 22$ TeV, the best-fit gluino pole mass is always much larger than the lower bound imposed.

sleptons are lighter than the first two, and (b) the gluino is lighter than the top squarks and sbottoms. In this case, the lower bound on the gluino mass is now of order 1–1.2 TeV, *assuming* the branching ratio $\mathrm{BR}(\tilde{g} \to t\bar{t}\tilde{\chi}_1^0) = 100\%$ or $\mathrm{BR}(\tilde{g} \to b\bar{b}\tilde{\chi}_1^0) = 100\%$ [48]. Although neither simplified model is appropriate for our model, we nevertheless impose a lower bound on the gluino pole mass in order to be roughly consistent with the latest LHC results.

In Fig. 3(a) we present the best χ^2 fits as a function of m_{16} for two values of the lower bound that we impose on the gluino pole mass, i.e., 850 and 1000 GeV. We note that χ^2 is relatively insensitive to these lower bounds on the gluino mass, although lower values of $M_{\tilde{g}}$ are slightly favored. The minimum χ^2 is found for $m_{16} = 20$ TeV, and χ^2 increases as m_{16} either decreases or increases. Features of the model, like the large A-terms and large $\tan\beta$, are favorable to obtain a Higgs mass in the range of 122–127 GeV as observed at the LHC. However, the largest contribution to χ^2 for lower values of m_{16} comes from the Higgs mass constraint (see Fig. 4).

As the lower bound on the gluino mass is increased to 2 or 3 TeV, we find that χ^2 dramatically increases [see Fig. 3(b)]. Note that this is predominantly due to the constraint from the light Higgs mass (Fig. 4). The simple explanation for this fact is that as the gluino mass increases the magnitude of A_t at M_{SUSY} also increases, due to the infrared fixed point. This has the effect of decreasing the light Higgs mass because now $X_t > \sqrt{6}M_{\mathrm{SUSY}}$, which goes beyond maximal mixing. As a consequence, there appears to be an upper bound on the gluino mass of order 2 TeV, which makes gluinos inevitably observable at the LHC at 14 TeV. However, as discussed earlier, the usual simplified models do not apply since gluinos decay with branching ratios $\tilde{g} \to t\bar{t}\tilde{\chi}^0_{(1,2)}$, $b\bar{b}\tilde{\chi}^0_{(1,2)}$, $t\bar{b}\tilde{\chi}^-_{(1,2)}$, $b\bar{t}\tilde{\chi}^+_{(1,2)}$, $g\tilde{\chi}^0_{(1,2,3,4)}$ which are all significant.

In Fig. 5(a) we give the best χ^2 fits for the third-family analysis as a function of the lower bound on the gluino mass and the value of m_{16}. In Fig. 5(b) we give the contours of constant gluino masses (roughly horizontal lines) and top squark masses (vertical lines).[9] Note, for values of $m_{16} \geq 20$ TeV, the best-fit gluino pole mass is always much larger than the lower bound imposed.

V. FULL THREE-FAMILY ANALYSIS

In this section we present the global χ^2 analysis for three families including all 24 arbitrary parameters. The χ^2 function includes 36 observables. We present our results for fixed values of m_{16} in Fig. 6 and in Tables V, VI, VII, VIII, and IX.

In Fig. 6 we give the best χ^2 fits for two different values of the lower bound on the gluino pole mass imposed in the analysis. Figures 3 and 6 have similar behavior. The value of χ^2 increases dramatically for values of $m_{16} \lesssim 15$ TeV. For larger values of $m_{16} \gtrsim 25$ TeV the increase is much slower. In the three-family analysis, the minimum χ^2 occurs around $m_{16} \approx 20$ TeV, just as in the third-family analysis. Moreover, the input parameters which minimize χ^2 in the third-family analysis also minimize χ^2 for the full three family analysis.

[9] In a recent analysis [49], the authors found an upper bound on the top-squark mass for good Yukawa unification. Their result is a consequence of the constraint $\mu < 1000$ GeV, in order to satisfy dark matter bounds. We do not make any such assumption and do not find an upper bound on the top-squark mass for $m_{16} \leq 30$ TeV.

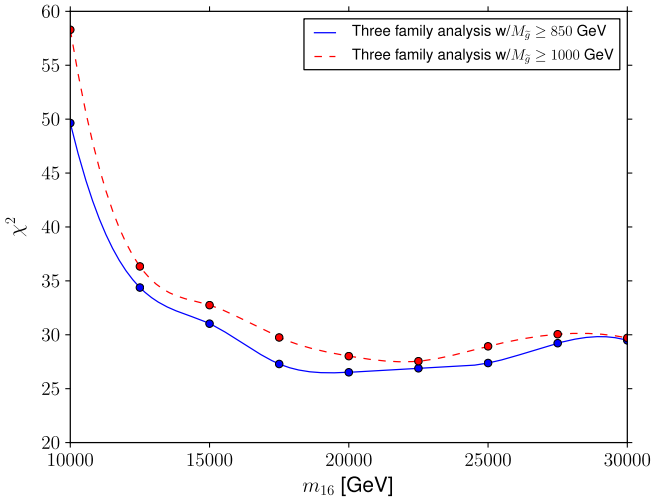

FIG. 6 (color online). χ^2 vs m_{16} for the full three-family analysis. χ^2 is very large for low values of $m_{16} \lesssim 15$ TeV. The blue (solid) and red (dashed) lines correspond to a lower bound on the gluino mass of 850 and 1000 GeV, respectively.

In Tables V, VI, VII, VIII, and IX we present the best χ^2 fits for values of $m_{16} = 10$, 15, 20, 25, and 30 TeV, respectively. The best fit overall comes for $m_{16} = 20$ TeV with $\chi^2/\text{d.o.f} \sim 2$ (see Table VII). Let us just comment on a few of the initial values of the parameters for this point. We find $\alpha_G \approx 1/26$, $M_G \approx 3 \times 10^{16}$ GeV, and $\epsilon_3 = -1.45\%$. The magnitude of the Yukawa couplings are hierarchical. As expected, we have $A_0 \approx -2m_{16}$, μ, $M_{1/2} \ll m_{16}$, and $\tan\beta \sim 50$. The average Higgs mass parameter and the relative splitting are given by $m_{10} \equiv \sqrt{(m_{H_u}^2 + m_{H_d}^2)/2} \approx 26$ TeV and $\Delta_{m_H}^2 \equiv (m_{H_d}^2 - m_{H_u}^2)/(2m_{10}^2) \approx 0.07$, respectively. The gravitino mass for this model is expected to be of order the largest scalar mass, i.e., $M_{3/2} \sim m_{10} \approx 26$ TeV. We used MICROMEGAS [50] to calculate the relic abundance for the benchmark points considered and found $\Omega^{\text{th}} = 22.2$ (10 TeV), $\Omega^{\text{th}} = 0.776$ (15 TeV), $\Omega^{\text{th}} = 70.0$ (20 TeV), $\Omega^{\text{th}} = 90.2$ (25 TeV), $\Omega^{\text{th}} = 123$ (30 TeV). This is a consequence of a purely bino-like lightest supersymmetric particle (LSP). In this case, a nonthermal process would be necessary to accommodate the observed dark matter abundance. Assuming the correct dark matter abundance, a bino LSP would not have been observed yet by direct detection methods, but should be observable by future detectors [51].

Let us now focus on the fit. Consider the observables with the largest pulls. Roughly half the contribution to χ^2 at this point comes from just two observables, namely m_d/m_s and $\sin 2\beta$. Our value of m_d/m_s is larger than the experimental value, and this implies that our value of $m_u/m_d \sim 0.9$ [see Eq. (19)]. We have allowed $|V_{ub}|$ to range over values consistent with both exclusive and inclusive measurements. We find that our fit is more consistent with exclusive measurements. Moreover, our fit value of $\sin 2\beta$ is at the 3σ lower bound allowed by the experiments. Otherwise we are able to fit an amazing array of experimental observables. The light Higgs mass is fit to within the ± 3 GeV theoretical uncertainty we have assigned. As for the neutrino mixing angle θ_{13} we obtain a value closer to 6°, rather than the present experimental value of approximately 9°. This may be a problem; however, it has been noticed recently that flavor-violating corrections to the Kähler potential can have a significant effect on θ_{13} without affecting the other larger mixing angles [52]. Our neutrino spectrum corresponds to the normal hierarchy. Note that the two large mixing angles are a consequence of a hierarchy in the right-handed neutrino masses.

In Table III we summarize the predictions for the SUSY spectrum given values of $m_{16} = 10$, 15, 20, 25, 30 TeV, respectively. We give the spectrum of the lightest squark, slepton, and gaugino masses, and the CP-odd Higgs mass M_A. The first- and second-generation squarks and sleptons all have mass of order m_{16}. Note that in order to fit the branching ratio $\text{BR}(B_s \to \mu^+\mu^-)$ with a large $\tan\beta$, we have $M_A \gg M_Z$. Thus we are in the decoupling limit where the light Higgs is predicted to couple to matter just like the Standard Model Higgs. Therefore, any deviation from this prediction would rule out our model. Finally, in Table IV we present results for yet-to-be-observed quantities, such as electric dipole moments of charged leptons, flavor-violating processes such as $\text{BR}(\mu \to e\gamma)$, and the CP-violating angle in the lepton sector, $\sin\delta$. The

TABLE IV. Predictions from the full three-family analysis. The dipole moments and branching ratios were calculated using SUSY_FLAVOR.

	Current limit	10 TeV	15 TeV	20 TeV	25 TeV	30 TeV
e EDM $\times 10^{28}$	$<10.5e$ cm	−0.224	−0.0408	−0.0173	−0.0113	−0.0084
μ EDM $\times 10^{28}$	$(-0.1 \pm 0.9) \times 10^9 e$ cm	34.6	6.23	3.04	1.77	1.20
τ EDM $\times 10^{28}$	$-0.220 - 0.45 \times 10^{12} e$ cm	−2.09	−0.394	−0.185	−0.109	−0.0732
$\text{BR}(\mu \to e\gamma) \times 10^{12}$	$<2.4e$ cm	5.09	1.23	0.211	0.0937	0.0447
$\text{BR}(\tau \to e\gamma) \times 10^{12}$	$<3.3 \times 10^4$ $e$cm	58.8	13.9	2.40	1.04	0.502
$\text{BR}(\tau \to \mu\gamma) \times 10^8$	$<4.4e$ cm	1.75	0.498	0.0837	0.0385	0.0182
$\sin\delta$		−0.60	−0.87	−0.27	−0.42	−0.53

value of $\sin\delta$ is close to zero and is thus consistent with tentative emerging hints for $\delta \simeq \pi$ [42]. We also find that the BR($\mu \to e\gamma$) may in fact be observable by the MEG experiment in a few years [53].

VI. SUMMARY AND CONCLUSIONS

We have performed a global χ^2 analysis of an SO(10) SUSY GUT times a $D_3 \times [\mathrm{U}(1) \times \mathbb{Z}_2 \times \mathbb{Z}_3]$ family symmetry. The model fits all fermion masses and mixing angles—as well as many flavor observables—quite well. The model has 24 arbitrary parameters which we use to fit 36 low-energy observables. Five of these parameters include: the soft SUSY-breaking masses; a universal squark and slepton mass, m_{16}; a universal cubic scalar coupling, A_0; a universal gaugino mass, $M_{1/2}$; and split Higgs up and down masses, m_{H_u}, m_{H_d}. The model has gauge coupling unification and top, bottom, τ, and ν_τ Yukawa unification at M_{GUT}. We have analyzed the model for the third family alone and then for three families. We have shown that the SUSY spectrum is predominantly determined by fitting the third family and light Higgs masses and the branching ratio BR($B_s \to \mu^+\mu^-$). In Tables V, VI, VII, VIII, and IX we give the best three-family fits for five different values of the universal scalar mass m_{16}. The best overall fit is found for $m_{16} \approx 20$ TeV. The SUSY spectrum for these best-fit points are given in Table III.

Our model makes several significant predictions.

(i) The first and second family of squarks and sleptons obtain mass of order m_{16}, while the third-family scalars are naturally much lighter. Then gluinos and the lightest chargino and neutralinos are always lighter than the third-family squarks and sleptons.

(ii) Due to Yukawa unification of the third family at the GUT scale we have $\tan\beta \approx 50$. In order to fit the branching ratio BR($B_s \to \mu^+\mu^-$) we find the CP-odd Higgs mass, $m_A \gg M_Z$. Hence we are in the decoupling limit and the light Higgs is predicted to be Standard Model-like.

(iii) In order to fit the light Higgs mass, we find an upper bound on the gluino mass, $M_{\tilde{g}} \sim 2$ TeV. Thus gluinos should be observable at LHC14.

(iv) No simplified model studied to date describes the relevant gluino decay branching ratios (see scenarios studied in Ref. [54]). Thus in order to constrain our theory we need both CMS and ATLAS to provide detailed bounds on the $pp \to \tilde{g}\,\tilde{g}$ production cross section times branching ratios for the many different two- and three-body decay modes, i.e., $\tilde{g} \to t\bar{t}\tilde{\chi}^0_{(1,2)}$, $b\bar{b}\tilde{\chi}^0_{(1,2)}$, $t\bar{b}\tilde{\chi}^-_{(1,2)}$, $b\bar{t}\tilde{\chi}^+_{(1,2)}$, and $g\tilde{\chi}^0_{(1,2,3,4)}$.[10]

(v) We find BR($\mu \to e\gamma$) $\sim 10^{-12}$–10^{-13} for values of $m_{16} = 15$–25 TeV. This may soon be observable at MEG [53].

(vi) We find the CP-violating parameter in the lepton sector, $\sin\delta \approx 0$, and the neutrinos obey a normal hierarchy.

(vii) Since the first two families of sleptons have mass of order m_{16} we are not able to fit the muon anomalous magnetic moment, $(g-2)_\mu$.

(viii) Our LSP is predominantly bino and thus, assuming a thermal calculation of the relic abundance, we find $\Omega_{\tilde{\chi}^0_1}$ too large.

(ix) The gravitino mass is naturally of order $\sqrt{2}m_{16}$ or for $m_{16} = 15$–25 TeV we have $m_{\tilde{G}} \sim 20$–35 TeV. Thus the the model may avoid the cosmological gravitino problem.

There is one obvious issue with the model regarding fine-tuning. We have not performed a detailed analysis of fine-tuning, but a rough measure is given by $\Delta = (\frac{\mu}{M_Z})^2 \sim 150$, corresponding to a fine-tuning of $1/\Delta$. As this is true for most of the surviving parameter space of the MSSM, at the moment we do not regard this as a serious problem. The question of electroweak fine-tuning in Yukawa unified models was recently studied in Ref. [55].

Let us now consider future directions. We will evaluate the gluino decay branching ratios in our model in order to compare to LHC data in a future work. In addition, we want to analyze other boundary conditions at the GUT scale consistent with gauge and Yukawa coupling unification. In particular, we will consider the "DR3" scheme [12] and also nonuniversal gaugino masses as discussed in Ref. [13], and study them with the combined predictive power of family symmetries. On the computational front, we would like to explore other methods to tackle the problem of finding a global minimum in a multidimensional parameter space.

ACKNOWLEDGMENTS

We are indebted to Radovan Dermíšek for his program and his valuable inputs in using it. We also thank Christopher Plumberg and Aditi Raval for their work in the early stages of the project. We acknowledge useful discussions with Athanasios Dedes, Chris Hill, Nazila Mahmoudi, and Janusz Rosiek. We thank Pietro Slavich for sharing their Higgs boson mass calculation routine. A. A. and S. R. received partial support for this work from DOE/ER/01545-896. A. W. acknowledges partial support from LabEx ENIGMASS and would like to thank the Ohio State University for their hospitality. We thank the Ohio Supercomputer Center and the Centre de Calcul de l'Institut National de Physique Nucléaire et Physique des Particules in Lyon for using their resources.

[10] In order for ATLAS or CMS to test our model, we would gladly provide an SLHA2 file specifying all the low-energy parameters of any of our benchmark points.

APPENDIX: BENCHMARK POINTS

TABLE V. Initial parameters for the benchmark point with $m_{16} = 10$ TeV: $(1/\alpha_G, M_G, \epsilon_3) = (25.42, 2.80 \times 10^{16}\,\text{GeV}, -2.20\%)$, $(\lambda, \lambda\epsilon, \sigma, \lambda\tilde{\epsilon}, \rho, \lambda\epsilon', \lambda\epsilon\xi) = (0.61, 0.031, 1.14, 0.0048, 0.071, -0.0019, 0.0038)$, $(\Phi_\sigma, \Phi_{\tilde{\epsilon}}, \Phi_\rho, \Phi_\xi) = (0.517, 0.625, 4.000, 3.497)$ rad, $(m_{16}, M_{1/2}, A_0, \mu(M_Z)) = (10000, 239, -20247, 791.13)$ GeV, $((m_{H_d}/m_{16})^2, (m_{H_u}/m_{16})^2, \tan\beta) = (1.95, 1.61, 49.42)$, $(M_{R_3}, M_{R_2}, M_{R_1}) = (3.2 \times 10^{13}\ \text{GeV}, 5.6 \times 10^{11}\ \text{GeV}, 0.9 \times 10^{10}\ \text{GeV})$.

Observable	Fit value	Exp. value	Pull	σ
M_Z	91.1876	91.1876	0.0000	0.4559
M_W	80.5581	80.3850	0.4305	0.4022
$1/\alpha_{\text{em}}$	136.3909	137.0360	0.9415	0.6852
$G_\mu \times 10^5$	1.1754	1.1664	0.7722	0.0117
α_3	0.1184	0.1184	0.0342	0.0009
M_t	173.9306	173.5000	0.3253	1.3238
$m_b(m_b)$	4.1719	4.1800	0.2213	0.0366
M_τ	1.7796	1.7768	0.3104	0.0089
$m_c(m_c)$	1.2782	1.2750	0.1246	0.0258
m_s	0.0962	0.0950	0.2437	0.0050
m_d/m_s	0.0710	0.0526	3.3115	0.0055
$1/Q^2$	0.0019	0.0019	0.2854	0.0001
M_μ	0.1056	0.1057	0.2011	0.0005
$M_e \times 10^4$	5.1137	5.1100	0.1450	0.0255
$\lvert V_{us}\rvert$	0.2248	0.2252	0.2886	0.0014
$\lvert V_{cb}\rvert$	0.0424	0.0406	0.8748	0.0020
$\lvert V_{ub}\rvert \times 10^3$	3.3462	3.7700	0.4985	0.8502
$\lvert V_{td}\rvert \times 10^3$	9.5185	8.4000	1.8597	0.6015
$\lvert V_{ts}\rvert$	0.0414	0.0429	0.5683	0.0026
$\sin 2\beta$	0.6357	0.6790	2.1346	0.0203
ϵ_K	0.0023	0.0022	0.2568	0.0002
$\Delta M_{Bs}/\Delta M_{Bd}$	59.6805	35.0600	3.5049	7.0246
$\Delta M_{Bd} \times 10^{13}$	3.5432	3.3370	0.3086	0.6682
$m_{21}^2 \times 10^5$	7.6408	7.5450	0.1754	0.5463
$m_{31}^2 \times 10^3$	2.6521	2.4800	0.8182	0.2104
$\sin^2\theta_{12}$	0.3297	0.3050	0.7041	0.0350
$\sin^2\theta_{23}$	0.6441	0.5050	0.8427	0.1650
$\sin^2\theta_{13}$	0.0128	0.0230	1.4585	0.0070
M_h	116.94	125.30	2.7265	3.0676
$\text{BR}(B \to X_s\gamma) \times 10^4$	3.9408	3.4300	0.3120	1.6374
$\text{BR}(B_s \to \mu^+\mu^-) \times 10^9$	2.3710	3.2000	0.5083	1.6308
$\text{BR}(B_d \to \mu^+\mu^-) \times 10^{10}$	1.7509	8.1000	0.0000	5.2559
$\text{BR}(B \to \tau\nu) \times 10^5$	7.1988	16.6000	1.0525	8.9320
$\text{BR}(B \to K^*\mu^+\mu^-)(\text{low}) \times 10^8$	5.4370	19.7000	1.1881	12.0051
$\text{BR}(B \to K^*\mu^+\mu^-)(\text{high}) \times 10^8$	7.8844	12.0000	0.5651	7.2835
$q_0^2(B \to K^*\mu^+\mu^-)$	4.8731	4.9000	0.0206	1.3009
Total χ^2			49.6463	

TABLE VI. Initial parameters for the benchmark point with $m_{16} = 15$ TeV: $(1/\alpha_G, M_G, \epsilon_3) = (25.50, 2.96 \times 10^{16}\ \text{GeV}, -2.40\%)$, $(\lambda, \lambda\epsilon, \sigma, \lambda\tilde{\epsilon}, \rho, \lambda\epsilon', \lambda\epsilon\xi) = (0.61, 0.031, 1.14, 0.0049, 0.070, -0.0019, 0.0037)$, $(\Phi_\sigma, \Phi_{\tilde{\epsilon}}, \Phi_\rho, \Phi_\xi) = (0.527, 0.635, 3.881, 3.429)$ rad, $(m_{16}, M_{1/2}, A_0, \mu(M_Z)) = (15000, 201, -30639, 513.07)$ GeV, $((m_{H_d}/m_{16})^2, (m_{H_u}/m_{16})^2, \tan\beta) = (1.97, 1.62, 49.59)$, $(M_{R_3}, M_{R_2}, M_{R_1}) = (4.2 \times 10^{13}\ \text{GeV}, 6.1 \times 10^{11}\ \text{GeV}, 1.0 \times 10^{10}\ \text{GeV})$.

Observable	Fit value	Exp. value	Pull	Sigma
M_Z	91.1876	91.1876	0.0000	0.4559
M_W	80.5671	80.3850	0.4527	0.4022
$1/\alpha_{\text{em}}$	136.4172	137.0360	0.9031	0.6852
$G_\mu \times 10^5$	1.1766	1.1664	0.8739	0.0117
α_3	0.1185	0.1184	0.1342	0.0009
M_t	173.5253	173.5000	0.0191	1.3238
$m_b(m_b)$	4.1903	4.1800	0.2813	0.0366
M_τ	1.7756	1.7768	0.1366	0.0089
$m_c(m_c)$	1.2613	1.2750	0.5312	0.0258
m_s	0.0964	0.0950	0.2766	0.0050
m_d/m_s	0.0686	0.0526	2.8819	0.0055
$1/Q^2$	0.0018	0.0019	0.4900	0.0001
M_μ	0.1056	0.1057	0.0748	0.0005
$M_e \times 10^4$	5.1135	5.1100	0.1386	0.0255
$\lvert V_{us}\rvert$	0.2243	0.2252	0.6542	0.0014
$\lvert V_{cb}\rvert$	0.0410	0.0406	0.1681	0.0020
$\lvert V_{ub}\rvert \times 10^3$	3.1115	3.7700	0.7745	0.8502
$\lvert V_{td}\rvert \times 10^3$	8.8886	8.4000	0.8124	0.6015
$\lvert V_{ts}\rvert$	0.0401	0.0429	1.0638	0.0026
$\sin 2\beta$	0.6220	0.6790	2.8094	0.0203
ϵ_K	0.0023	0.0022	0.1079	0.0002
$\Delta M_{Bs}/\Delta M_{Bd}$	37.6694	35.0600	0.3715	7.0246
$\Delta M_{Bd} \times 10^{13}$	4.0059	3.3370	1.0010	0.6682
$m_{21}^2 \times 10^5$	7.5155	7.5450	0.0540	0.5463
$m_{31}^2 \times 10^3$	2.5097	2.4800	0.1413	0.2104
$\sin^2\theta_{12}$	0.2994	0.3050	0.1600	0.0350
$\sin^2\theta_{23}$	0.7414	0.5050	1.4323	0.1650
$\sin^2\theta_{13}$	0.0147	0.0230	1.1908	0.0070
M_h	122.21	125.30	1.0080	3.0676
$\text{BR}(B \to X_s\gamma) \times 10^4$	3.5456	3.4300	0.0706	1.6374
$\text{BR}(B_s \to \mu^+\mu^-) \times 10^9$	4.3688	3.2000	0.7167	1.6308
$\text{BR}(B_d \to \mu^+\mu^-) \times 10^{10}$	1.3486	8.1000	0.0000	5.2559
$\text{BR}(B \to \tau\nu) \times 10^5$	6.2875	16.6000	1.1546	8.9320
$\text{BR}(B \to K^*\mu^+\mu^-)(\text{low} \times 10^8$	5.0499	19.7000	1.2203	12.0051
$\text{BR}(B \to K^*\mu^+\mu^-)(\text{high}) \times 10^8$	7.5449	12.0000	0.6117	7.2835
$q_0^2(B \to K^*\mu^+\mu^-)$	4.5922	4.9000	0.2366	1.3009
Total χ^2			31.0266	

TABLE VII. Initial parameters for the benchmark point with $m_{16} = 20$ TeV: $(1/\alpha_G, M_G, \epsilon_3) = (25.90, 3.13 \times 10^{16}\ \text{GeV}, -1.45\%)$, $(\lambda, \lambda\epsilon, \sigma, \lambda\tilde{\epsilon}, \rho, \lambda\epsilon', \lambda\epsilon\xi) = (0.60, 0.031, 1.14, 0.0049, 0.070, -0.0019, 0.0038)$, $(\Phi_\sigma, \Phi_{\tilde{\epsilon}}, \Phi_\rho, \Phi_\xi) = (0.533, 0.548, 3.936, 3.508)$ rad, $(m_{16}, M_{1/2}, A_0, \mu(M_Z)) = (20000, 168, -41087, 1163.25)$ GeV, $((m_{H_d}/m_{16})^2, (m_{H_u}/m_{16})^2, \tan\beta) = (1.85, 1.61, 49.82)$, $(M_{R_3}, M_{R_2}, M_{R_1}) = (3.2 \times 10^{13}\ \text{GeV}, 6.1 \times 10^{11}\ \text{GeV}, 0.9 \times 10^{10}\ \text{GeV})$.

Observable	Fit value	Exp. value	Pull	Sigma
M_Z	91.1876	91.1876	0.0000	0.4559
M_W	80.5452	80.3850	0.3982	0.4022
$1/\alpha_{\text{em}}$	137.0725	137.0360	0.0533	0.6852
$G_\mu \times 10^5$	1.1713	1.1664	0.4250	0.0117
α_3	0.1184	0.1184	0.0467	0.0009
M_t	174.0184	173.5000	0.3916	1.3238
$m_b(m_b)$	4.1849	4.1800	0.1334	0.0366
M_τ	1.7755	1.7768	0.1462	0.0089
$m_c(m_c)$	1.2547	1.2750	0.7876	0.0258
m_s	0.0964	0.0950	0.2807	0.0050
m_d/m_s	0.0692	0.0526	2.9891	0.0055
$1/Q^2$	0.0018	0.0019	0.4749	0.0001
M_μ	0.1056	0.1057	0.1049	0.0005
$M_e \times 10^4$	5.1122	5.1100	0.0862	0.0255
$\lvert V_{us}\rvert$	0.2243	0.2252	0.5964	0.0014
$\lvert V_{cb}\rvert$	0.0415	0.0406	0.4511	0.0020
$\lvert V_{ub}\rvert \times 10^3$	3.2023	3.7700	0.6678	0.8502
$\lvert V_{td}\rvert \times 10^3$	8.9819	8.4000	0.9675	0.6015
$\lvert V_{ts}\rvert$	0.0407	0.0429	0.8518	0.0026
$\sin 2\beta$	0.6304	0.6790	2.3959	0.0203
ϵ_K	0.0023	0.0022	0.3823	0.0002
$\Delta M_{Bs}/\Delta M_{Bd}$	39.4933	35.0600	0.6311	7.0246
$\Delta M_{Bd} \times 10^{13}$	3.9432	3.3370	0.9072	0.6682
$m_{21}^2 \times 10^5$	7.5126	7.5450	0.0593	0.5463
$m_{31}^2 \times 10^3$	2.4828	2.4800	0.0135	0.2104
$\sin^2\theta_{12}$	0.2949	0.3050	0.2880	0.0350
$\sin^2\theta_{23}$	0.5156	0.5050	0.0640	0.1650
$\sin^2\theta_{13}$	0.0131	0.0230	1.4134	0.0070
M_h	124.07	125.30	0.4010	3.0676
$\text{BR}(B \to X_s\gamma) \times 10^4$	3.4444	3.4300	0.0088	1.6374
$\text{BR}(B_s \to \mu^+\mu^-) \times 10^9$	1.6210	3.2000	0.9682	1.6308
$\text{BR}(B_d \to \mu^+\mu^-) \times 10^{10}$	1.0231	8.1000	0.0000	5.2559
$\text{BR}(B \to \tau\nu) \times 10^5$	6.3855	16.6000	1.1436	8.9320
$\text{BR}(B \to K^*\mu^+\mu^-)(\text{low}) \times 10^8$	5.1468	19.7000	1.2123	12.0051
$\text{BR}(B \to K^*\mu^+\mu^-)(\text{high}) \times 10^8$	7.7469	12.0000	0.5839	7.2835
$q_0^2(B \to K^*\mu^+\mu^-)$	4.5168	4.9000	0.2945	1.3009
Total χ^2			26.5812	

TABLE VIII. Initial parameters for the benchmark point with $m_{16} = 25$ TeV: $(1/\alpha_G, M_G, \epsilon_3) = (25.83, 4.17 \times 10^{16}\,\text{GeV}, -2.55\%)$, $(\lambda, \lambda\epsilon, \sigma, \lambda\tilde{\epsilon}, \rho, \lambda\epsilon', \lambda\epsilon\xi) = (0.61, 0.031, 1.17, 0.0049, 0.070, -0.0019, 0.0037)$, $(\Phi_\sigma, \Phi_{\tilde{\epsilon}}, \Phi_\rho, \Phi_\xi) = (0.513, 0.542, 3.969, 3.503)\,\text{rad}$, $(m_{16}, M_{1/2}, A_0, \mu(M_Z)) = (25000, 158, -51365, 1348)\,\text{GeV}$, $((m_{H_d}/m_{16})^2, (m_{H_u}/m_{16})^2, \tan\beta) = (1.86, 1.61, 49.98)$, $(M_{R_3}, M_{R_2}, M_{R_1}) = (3.2 \times 10^{13}\,\text{GeV}, 6.1 \times 10^{11}\,\text{GeV}, 0.9 \times 10^{10}\,\text{GeV})$.

Observable	Fit value	Exp. value	Pull	Sigma
M_Z	91.1876	91.1876	0.0000	0.4559
M_W	80.6192	80.3850	0.5824	0.4022
$1/\alpha_{\text{em}}$	137.1624	137.0360	0.1844	0.6852
$G_\mu \times 10^5$	1.1754	1.1664	0.7749	0.0117
α_3	0.1185	0.1184	0.0889	0.0009
M_t	174.5241	173.5000	0.7735	1.3238
$m_b(m_b)$	4.1789	4.1800	0.0307	0.0366
M_τ	1.7761	1.7768	0.0800	0.0089
$m_c(m_c)$	1.2529	1.2750	0.8559	0.0258
m_s	0.0963	0.0950	0.2652	0.0050
m_d/m_s	0.0702	0.0526	3.1726	0.0055
$1/Q^2$	0.0019	0.0019	0.3379	0.0001
M_μ	0.1057	0.1057	0.1533	0.0005
$M_e \times 10^4$	5.1102	5.1100	0.0083	0.0255
$\lvert V_{us}\rvert$	0.2244	0.2252	0.5407	0.0014
$\lvert V_{cb}\rvert$	0.0411	0.0406	0.2090	0.0020
$\lvert V_{ub}\rvert \times 10^3$	3.1806	3.7700	0.6933	0.8502
$\lvert V_{td}\rvert \times 10^3$	8.9530	8.4000	0.9193	0.6015
$\lvert V_{ts}\rvert$	0.0402	0.0429	1.0358	0.0026
$\sin 2\beta$	0.6318	0.6790	2.3268	0.0203
ϵ_K	0.0024	0.0022	0.8902	0.0002
$\Delta M_{Bs}/\Delta M_{Bd}$	35.1576	35.0600	0.0139	7.0246
$\Delta M_{Bd} \times 10^{13}$	4.1075	3.3370	1.1531	0.6682
$m_{21}^2 \times 10^5$	7.5325	7.5450	0.0229	0.5463
$m_{31}^2 \times 10^3$	2.4814	2.4800	0.0066	0.2104
$\sin^2\theta_{12}$	0.2978	0.3050	0.2069	0.0350
$\sin^2\theta_{23}$	0.5109	0.5050	0.0358	0.1650
$\sin^2\theta_{13}$	0.0140	0.0230	1.2789	0.0070
M_h	125.21	125.30	0.0293	3.0676
$\text{BR}(B \to X_s\gamma) \times 10^4$	3.4074	3.4300	0.0138	1.6374
$\text{BR}(B_s \to \mu^+\mu^-) \times 10^9$	2.6112	3.2000	0.3610	1.6308
$\text{BR}(B_d \to \mu^+\mu^-) \times 10^{10}$	1.0779	8.1000	0.0000	5.2559
$\text{BR}(B \to \tau\nu) \times 10^5$	6.4123	16.6000	1.1406	8.9320
$\text{BR}(B \to K^*\mu^+\mu^-)(\text{low}) \times 10^8$	5.0511	19.7000	1.2202	12.0051
$\text{BR}(B \to K^*\mu^+\mu^-)(\text{high}) \times 10^8$	7.6223	12.0000	0.6010	7.2835
$q_0^2(B \to K^*\mu^+\mu^-)$	4.4839	4.9000	0.3198	1.3009
Total χ^2			27.9288	

TABLE IX. Initial parameters for the benchmark point with $m_{16} = 30$ TeV: $(1/\alpha_G, M_G, \epsilon_3) = (25.86, 4.36 \times 10^{16}\ \text{GeV}, -2.81\%)$, $(\lambda, \lambda\epsilon, \sigma, \lambda\tilde{\epsilon}, \rho, \lambda\epsilon', \lambda\epsilon\xi) = (0.62, 0.031, 1.18, 0.0050, 0.069, -0.0020, 0.0037)$, $(\Phi_\sigma, \Phi_{\tilde{\epsilon}}, \Phi_\rho, \Phi_\xi) = (0.507, 0.534, 4.005, 3.514)$ rad, $(m_{16}, M_{1/2}, A_0, \mu(M_Z)) = (30000, 161, -61640, 1647)$ GeV, $((m_{H_d}/m_{16})^2, (m_{H_u}/m_{16})^2, \tan\beta) = (1.86, 1.63, 50.15)$, $(M_{R_3}, M_{R_2}, M_{R_1}) = (3.2 \times 10^{13}\ \text{GeV}, 6.4 \times 10^{11}\ \text{GeV}, 0.9 \times 10^{10}\ \text{GeV})$.

Observable	Fit value	Exp. value	Pull	Sigma
M_Z	91.1876	91.1876	0.0000	0.4559
M_W	80.6519	80.3850	0.6637	0.4022
$1/\alpha_{\text{em}}$	137.0422	137.0360	0.0091	0.6852
$G_\mu \times 10^5$	1.1785	1.1664	1.0410	0.0117
α_3	0.1187	0.1184	0.2850	0.0009
M_t	175.0383	173.5000	1.1620	1.3238
$m_b(m_b)$	4.1782	4.1800	0.0484	0.0366
M_τ	1.7764	1.7768	0.0419	0.0089
$m_c(m_c)$	1.2504	1.2750	0.9540	0.0258
m_s	0.0972	0.0950	0.4362	0.0050
m_d/m_s	0.0712	0.0526	3.3536	0.0055
$1/Q^2$	0.0019	0.0019	0.3029	0.0001
M_μ	0.1058	0.1057	0.1928	0.0005
$M_e \times 10^4$	5.1097	5.1100	0.0125	0.0255
$\lvert V_{us}\rvert$	0.2244	0.2252	0.5324	0.0014
$\lvert V_{cb}\rvert$	0.0405	0.0406	0.0988	0.0020
$\lvert V_{ub}\rvert \times 10^3$	3.1793	3.7700	0.6947	0.8502
$\lvert V_{td}\rvert \times 10^3$	8.9071	8.4000	0.8431	0.6015
$\lvert V_{ts}\rvert$	0.0396	0.0429	1.2682	0.0026
$\sin 2\beta$	0.6380	0.6790	2.0207	0.0203
ϵ_K	0.0022	0.0022	0.0877	0.0002
$\Delta M_{Bs}/\Delta M_{Bd}$	34.0021	35.0600	0.1506	7.0246
$\Delta M_{Bd} \times 10^{13}$	4.1018	3.3370	1.1445	0.6682
$m_{21}^2 \times 10^5$	7.5705	7.5450	0.0467	0.5463
$m_{31}^2 \times 10^3$	2.4783	2.4800	0.0081	0.2104
$\sin^2\theta_{12}$	0.3057	0.3050	0.0213	0.0350
$\sin^2\theta_{23}$	0.5036	0.5050	0.0087	0.1650
$\sin^2\theta_{13}$	0.0130	0.0230	1.4280	0.0070
M_h	125.88	125.30	0.1876	3.0676
$\text{BR}(B \to X_s\gamma) \times 10^4$	3.3931	3.4300	0.0225	1.6374
$\text{BR}(B_s \to \mu^+\mu^-) \times 10^9$	2.6139	3.2000	0.3594	1.6308
$\text{BR}(B_d \to \mu^+\mu^-) \times 10^{10}$	1.0748	8.1000	0.0000	5.2559
$\text{BR}(B \to \tau\nu) \times 10^5$	6.4081	16.6000	1.1411	8.9320
$\text{BR}(B \to K^*\mu^+\mu^-)(\text{low}) \times 10^8$	4.9279	19.7000	1.2305	12.0051
$\text{BR}(B \to K^*\mu^+\mu^-)(\text{high}) \times 10^8$	7.4423	12.0000	0.6257	7.2835
$q_0^2(B \to K^*\mu^+\mu^-)$	4.4707	4.9000	0.3300	1.3009
Total χ^2			29.4783	

[1] S. Dimopoulos, S. Raby, and F. Wilczek, Phys. Rev. D **24**, 1681 (1981).
[2] S. Dimopoulos and H. Georgi, Nucl. Phys. **B193**, 150 (1981).
[3] L. E. Ibanez and G. G. Ross, Phys. Lett. **105B**, 439 (1981).
[4] N. Sakai, Z. Phys. C **11**, 153 (1981).
[5] M. Einhorn and D. Jones, Nucl. Phys. **B196**, 475 (1982).
[6] W. J. Marciano and G. Senjanovic, Phys. Rev. D **25**, 3092 (1982).
[7] T. Blazek, R. Dermisek, and S. Raby, Phys. Rev. Lett. **88**, 111804 (2002).
[8] H. Baer and J. Ferrandis, Phys. Rev. Lett. **87**, 211803 (2001).
[9] T. Blazek, R. Dermisek, and S. Raby, Phys. Rev. D **65**, 115004 (2002).
[10] K. Tobe and J. D. Wells, Nucl. Phys. **B663**, 123 (2003).
[11] D. Auto, H. Baer, C. Balazs, A. Belyaev, J. Ferrandis, and X. Tata, J. High Energy Phys. 06 (2003) 023.
[12] H. Baer, S. Kraml, and S. Sekmen, J. High Energy Phys. 09 (2009) 005.
[13] M. Badziak, M. Olechowski, and S. Pokorski, J. High Energy Phys. 08 (2011) 147.
[14] H. Baer, S. Kraml, S. Sekmen, and H. Summy, J. High Energy Phys. 10 (2008) 079.
[15] H. Baer, S. Raza, and Q. Shafi, Phys. Lett. B **712**, 250 (2012).
[16] R. Dermisek and S. Raby, Phys. Lett. B **622**, 327 (2005).
[17] R. Dermisek, M. Harada, and S. Raby, Phys. Rev. D **74**, 035011 (2006).
[18] M. Albrecht, W. Altmannshofer, A. J. Buras, D. Guadagnoli, and D. M. Straub, J. High Energy Phys. 10 (2007) 055.
[19] L. J. Hall, R. Rattazzi, and U. Sarid, Phys. Rev. D **50**, 7048 (1994).
[20] M. S. Carena, M. Olechowski, S. Pokorski, and C. Wagner, Nucl. Phys. **B426**, 269 (1994).
[21] T. Blazek, S. Raby, and S. Pokorski, Phys. Rev. D **52**, 4151 (1995).
[22] R. Dermisek, S. Raby, L. Roszkowski, and R. R. De Austri, J. High Energy Phys. 04 (2003) 037.
[23] R. Dermisek, S. Raby, L. Roszkowski, and R. R. de Austri, J. High Energy Phys. 09 (2005) 029.
[24] H. Baer, S. Kraml, S. Sekmen, and H. Summy, J. High Energy Phys. 03 (2008) 056.
[25] J. A. Bagger, J. L. Feng, N. Polonsky, and R.-J. Zhang, Phys. Lett. B **473**, 264 (2000).
[26] C. Froggatt and H. B. Nielsen, Nucl. Phys. **B147**, 277 (1979).
[27] N. Arkani-Hamed and H. Murayama, Phys. Rev. D **56**, R6733 (1997).
[28] N. Bernal, A. Djouadi, and P. Slavich, J. High Energy Phys. 07 (2007) 016.
[29] D. M. Pierce, J. A. Bagger, K. T. Matchev, and R.-j. Zhang, Nucl. Phys. **B491**, 3 (1997).
[30] P. H. Chankowski, Z. Pluciennik, and S. Pokorski, Nucl. Phys. **B439**, 23 (1995).
[31] J. Beringer *et al.* (Particle Data Group), Phys. Rev. D **86**, 010001 (2012).
[32] CMS Collaboration, Phys. Lett. B **716**, 30 (2012).
[33] G. Aad *et al.* (ATLAS Collaboration), Phys. Lett. B **716**, 1 (2012).
[34] W. Altmannshofer, D. Guadagnoli, S. Raby, and D. M. Straub, Phys. Lett. B **668**, 385 (2008).
[35] B. Allanach, Comput. Phys. Commun. **143**, 305 (2002).
[36] Heavy Flavor Averaging Group, http://www.slac.stanford.edu/xorg/hfag/.
[37] C. G. Garcia, M. Maltoni, T. Schwetz, and J. Salvado (NuFIT Collaboration), Three-neutrino results after neutrino 2012 conference v1.0., http://www.nu-fit.org.
[38] LHCb Collaboration, Report No. LHCb-CONF-2012-008, http://cdsweb.cern.ch/record/1427691.
[39] LHCb Collaboration, Phys. Rev. Lett. **110**, 021801 (2013).
[40] F. An *et al.* (DAYA-BAY Collaboration), Phys. Rev. Lett. **108**, 171803 (2012).
[41] J. Ahn *et al.* (RENO Collaboration), Phys. Rev. Lett. **108**, 191802 (2012).
[42] G. Fogli, E. Lisi, A. Marrone, D. Montanino, A. Palazzo, and A. M. Rotunno, Phys. Rev. D **86**, 013012 (2012).
[43] M. Gonzalez-Garcia, M. Maltoni, J. Salvado, and T. Schwetz, J. High Energy Phys. 12 (2012) 123.
[44] A. Crivellin, J. Rosiek, P. Chankowski, A. Dedes, S. Jager, and P. Tanedo, arXiv:1203.5023.
[45] F. Mahmoudi, Comput. Phys. Commun. **178**, 745 (2008).
[46] F. Mahmoudi, Comput. Phys. Commun. **180**, 1579 (2009).
[47] F. James and M. Roos, Comput. Phys. Commun. **10**, 343 (1975).
[48] CMS Collaboration, Report No. CMS-SUS-12-028.
[49] G. Elor, L. J. Hall, D. Pinner, and J. T. Ruderman, J. High Energy Phys. 10 (2012) 111.
[50] G. Belanger, F. Boudjema, A. Pukhov, and A. Semenov, Nuovo Cimento Soc. Ital. Fis. **033N2C**, 111 (2010).
[51] C. Cheung, L. J. Hall, D. Pinner, and J. T. Ruderman, arXiv:1211.4873.
[52] M.-C. Chen, M. Fallbacher, M. Ratz, and C. Staudt, arXiv:1208.2947.
[53] S. Mihara (MEG Collaboration), AIP Conf. Proc. **1467**, 62 (2012).
[54] M. Toharia and J. D. Wells, J. High Energy Phys. 02 (2006) 015.
[55] H. Baer, S. Kraml, and S. Kulkarni, arXiv:1208.3039.